Supplementary Information For:

A Cd(II)-organic framework as a highly sensitive and rapid fluorometric sensor for ascorbic acid in aqueous medium

Aniruddha Das,[a®] Subhrajyoti Ghosh,[a®] Laurens Bourda,[b] Mostakim SK,[a] Kaustuv Banerjee,[a] Kristof Van Hecke, [b] Shyam Biswas[a*]

[a]Department of Chemistry, Indian Institute of Technology Guwahati, Guwahati, 781039 Assam, India. E-mail: sbiswas@iitg.ernet.in

[b]XStruct, Department of Chemistry, Ghent University, Krijgslaan 281 S3, 9000 Ghent, Belgium

* To whom correspondence should be addressed. E-mail: sbiswas@iitg.ac.in; Tel: 91-3612583309.

Materials and Characterization Methods:
The 2-((pyridin-4-ylmethyl)amino)terephthalic acid (H_2BDC-NH-CH_2-Py) linker was synthesized and characterized (Figures S1-S3, Supporting Information) following the procedure described below. All the chemicals were purchased from commercial sources and used without further purification. Fourier transform infrared (FT-IR) spectroscopy data were recorded in the range of 400-4000 cm^{-1} at room temperature with a Perkin Elmer Spectrum Two FT-IR spectrometer. The following indications were used to indicate the corresponding absorption bands: very strong (vs), strong (s), medium (m), weak (w), shoulder (sh) and broad (br). Thermogravimetric (TG) experiments were carried out with a heating rate of 10 °C min^{-1} under argon atmosphere using using a SDT Q600 thermogravimetric analyzer. XRPD data were collected in transmission mode using a Bruker D2 Phaser X-ray diffractometer (30 kV, 10 mA) using Cu-Kα (λ = 1.5406 Å) radiation. Specific surface area for N_2 sorption was measured on a Quantachrome Autosorb iQMP gas sorption analyzer at -196 °C. The compound was activated at 80 °C for 6 h under dynamic vacuum. Fluorescence emission studies were performed at room temperature using a HORIBA JOBIN YVON Fluoromax-4 spectrofluorometer. Fluorescence lifetimes were measured using a time-correlated single-photon counting (TCSPC) method on an Edinburgh Instrument Life-Spec II instrument. DFT calculations were carried out with the Gaussian 09 package using the B3LYP/6-31G basis set.

Preparation of IITG-6a Suspension for Fluorescence Sensing Experiments:
2 mg of **IITG-6a** was taken in 3 mL of milli-Q water into a 5 mL glass vial and it was converted to a suspension by sonicating for 1 h. The suspension was kept at ambient condition for 24 h to achieve a stable suspension before fluorescence experiments.

Fluorescence Sensing Experiments:
100 μL of aqueous suspension of **IITG-6a** was taken in a 5 mL quartz cuvette containing 2900 μL milli-Q water. Afterward, 10 mM aqueous solution of ascorbic acid (AA) was added to it in stepwise manner (50 μL in each step, total 200 μL). The fluorescence spectra were recorded before and after addition of AA. For the time dependent fluorescence experiment, a total volume of 200 μL of 10 mM AA was added at a time to the MOF suspension and the fluorescence spectra were recorded after every 60 s up to 300 s. The solution was excited at 350 nm and emission spectra were recorded in the range of 390 to 600 nm.

Preparation of AA-Spiked Urine Sample:
At first, 10 mL fresh urine of a healthy human was stored. Afterward, 500 mL of concentrated nitric acid was added to it and centrifuged for 10 min at a rate of 2500 rpm. The supernatant obtained after centrifugation was collected and diluted with milli-Q water to a concentration of 100 times that of the original volume. After that, an adequate quantity of AA was added to the urine sample to make the AA concentration in the urine sample as 10 mM.

Single-Crystal X-ray Diffraction:
For determining the structure of **IITG-6**, X-ray intensity data were collected at 100 K on a Rigaku Oxford Diffraction Supernova Dual Source (Cu at zero) diffractometer equipped with an Atlas CCD detector using ω scans and MoKα (λ = 0.71073 Å) radiation. The images were

interpreted and integrated with the program CrysAlisPro.[1] Using Olex2,[2] the structure was solved by direct methods using the ShelXT structure solution program and refined by full-matrix least-squares on F^2 using the ShelXL program package.[3, 4] Non-hydrogen atoms were anisotropically refined, and the hydrogen atoms in the riding mode with isotropic temperature factors were fixed at 1.2 times U(eq) of the parent atoms (1.5 times for methyl groups). The structure was refined as a 2-component inversion twin.

CCDC 2164197 contains the supplementary crystallographic data for this paper and can be obtained free of charge from The Cambridge Crystallographic Data Centre via www.ccdc.cam.ac.uk/structures."

Synthesis of H_2BDC-NH-CH_2-Py Linker:

The below-mentioned synthetic procedure was followed during the synthesis of the H_2BDC-NHCH_2-Py linker. 2-((pyridin-4-ylmethylene)amino)terephthalic acid (1.60 g, 6 mmol) was dissolved in 50 mL of DMF and stirred at room temperature until complete dissolution was achieved. After that, $NaBH_3CN$ (0.60 g, 9.00 mmol) was added to the mixture at 0 °C and kept under stirring conditions at 0 °C for 6 h. After 6 h, the reaction mixture was poured onto crushed ice in a 250 mL beaker and kept for 5 h to achieve complete precipitation of the yellow-colored product. Finally, the precipitate was collected by vacuum filtration, followed by washing with sufficient amount of water and drying in a conventional oven at 80 °C for 12 h. Yield: 0.8 g (2.93 mmol, 50%). ^{1}H NMR (400 MHz, DMSO-d_6): δ = 8.62 (d, 2H), 7.94 (d, 1H), 7.78 (d, 1H), 7.15 (dd, 1H), 6.98 (d, 1H), 4.82 (s, 2H) ppm. ^{13}C NMR (100 MHz, DMSO-d_6): δ = 169.79, 167.31, 157.45, 150.00, 147.62, 136.26, 132.73, 125.20, 116.18, 114.83, 112.45 ppm. ESI-MS (m/z): 273.08 for $(M+H)^+$ ion (M = mass of H_2BDC-$C_6H_7N_2$ linker). In Figures S1-S3 (Supporting Information), the NMR and mass spectra for the H_2BDC-NH-CH_2-Py linker are shown.

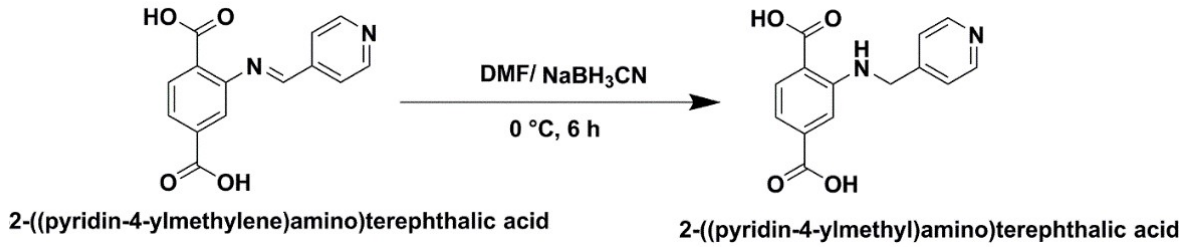

Scheme S1. Reaction scheme for the preparation of H_2BDC-NH-CH_2-Py linker.

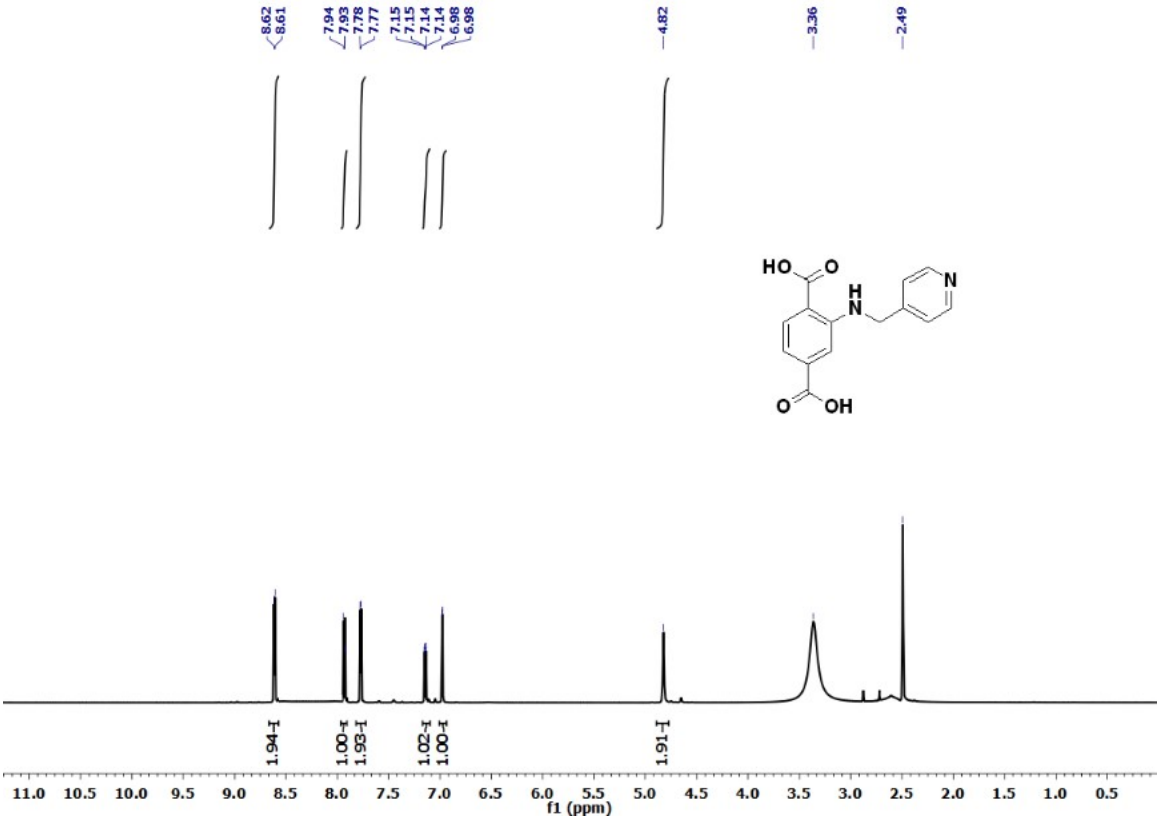

Fig. S1. ^{1}H NMR spectrum of the $H_2BDC\text{-}NH\text{-}CH_2\text{-}Py$ linker in DMSO-d_6.

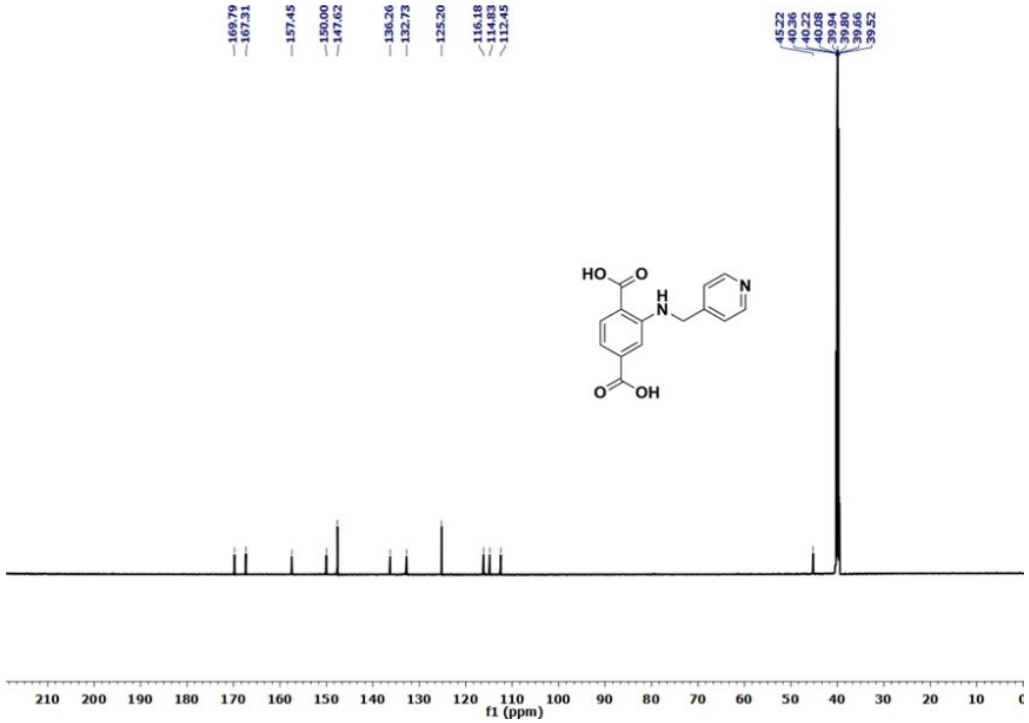

Fig. S2. ^{13}C NMR spectrum of the $H_2BDC\text{-}NH\text{-}CH_2\text{-}Py$ linker in DMSO-d_6.

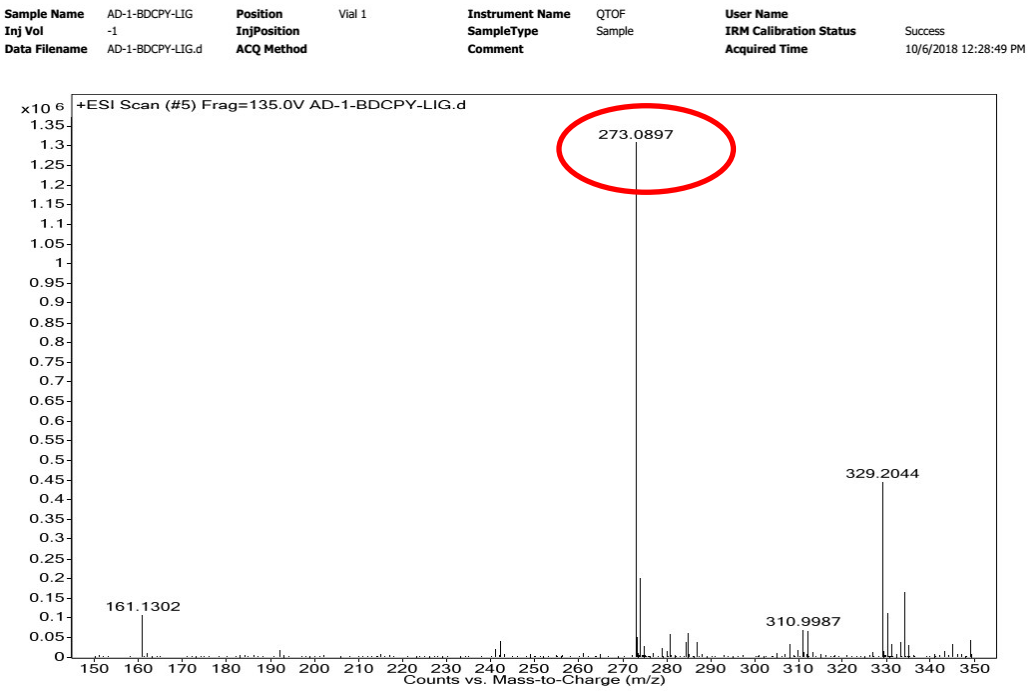

Fig. S3. ESI-MS spectrum of the H_2BDC-NH-CH_2-Py linker in methanol. The spectrum shows m/z (positive ion mode) peak at 273.08, which corresponds to $(M+H)^+$ ion (M = mass of H_2BDC-NH-CH_2-Py linker).

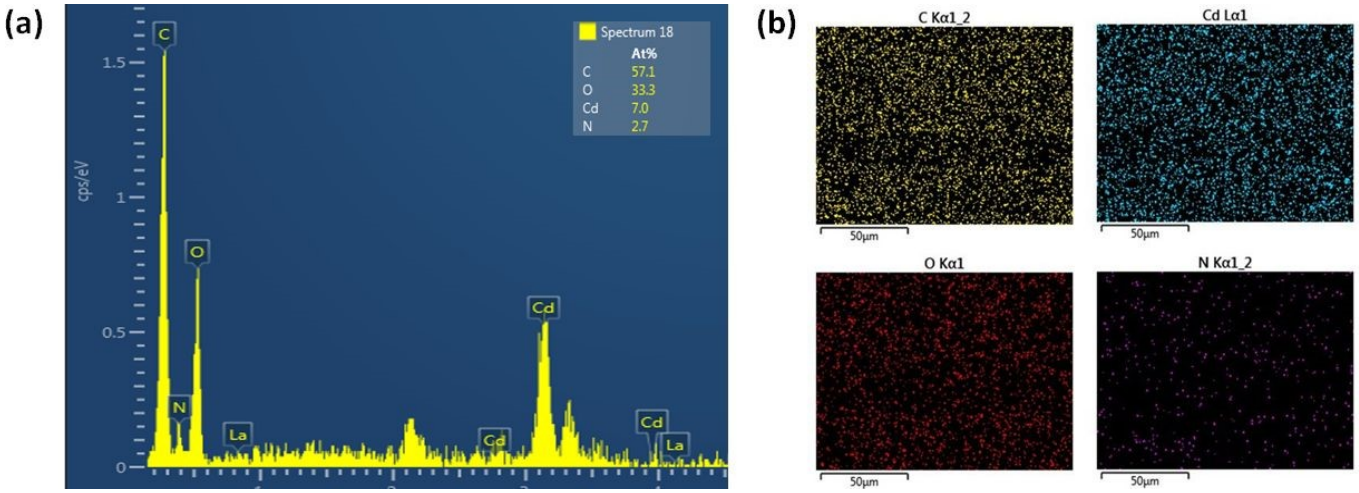

Fig. S4. EDX spectra and elemental mapping of **IITG-6**.

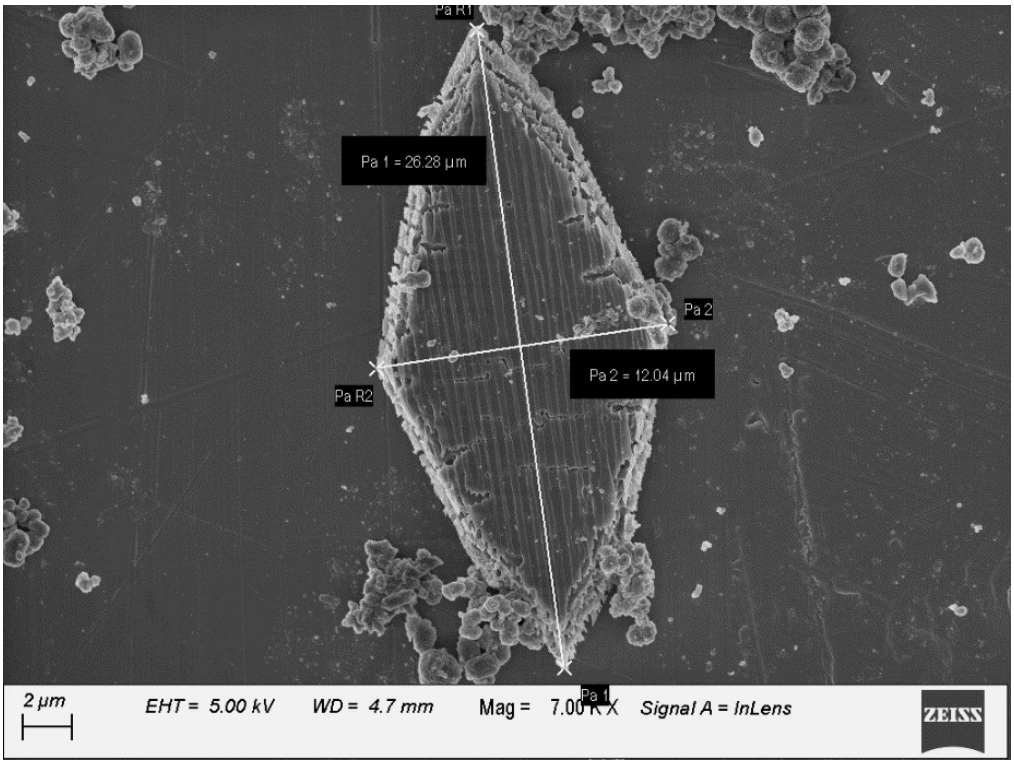

Fig. S5. FE-SEM images of **IITG-6**.

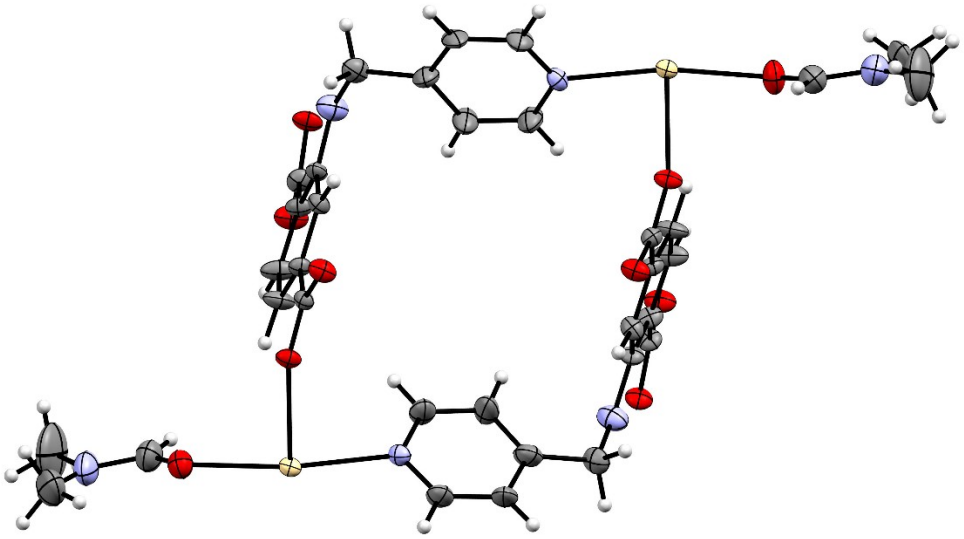

Fig. S6. Asymmetric unit of **IITG-6** (thermal displacement ellipsoids are shown at 50% probability level). Color code: hydrogen (white), oxygen (red), carbon (gray), nitrogen (light blue), cadmium (light yellow).

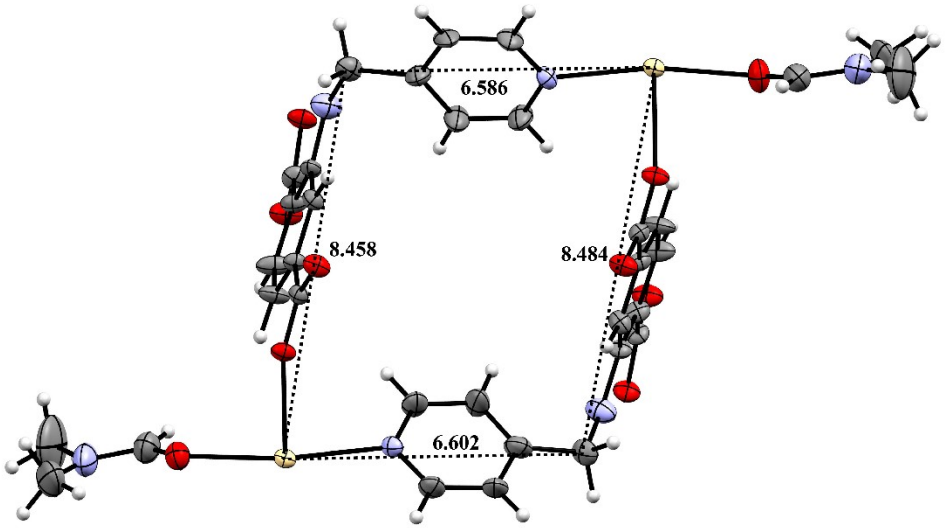

Fig. S7. A rhomboidal box having formula $Cd_2(\mathbf{H_2BDC\text{-}NH\text{-}CH_2\text{-}Py})_2$ of **IITG-6** with dimensions of 8.5 × 6.6 Å^2.

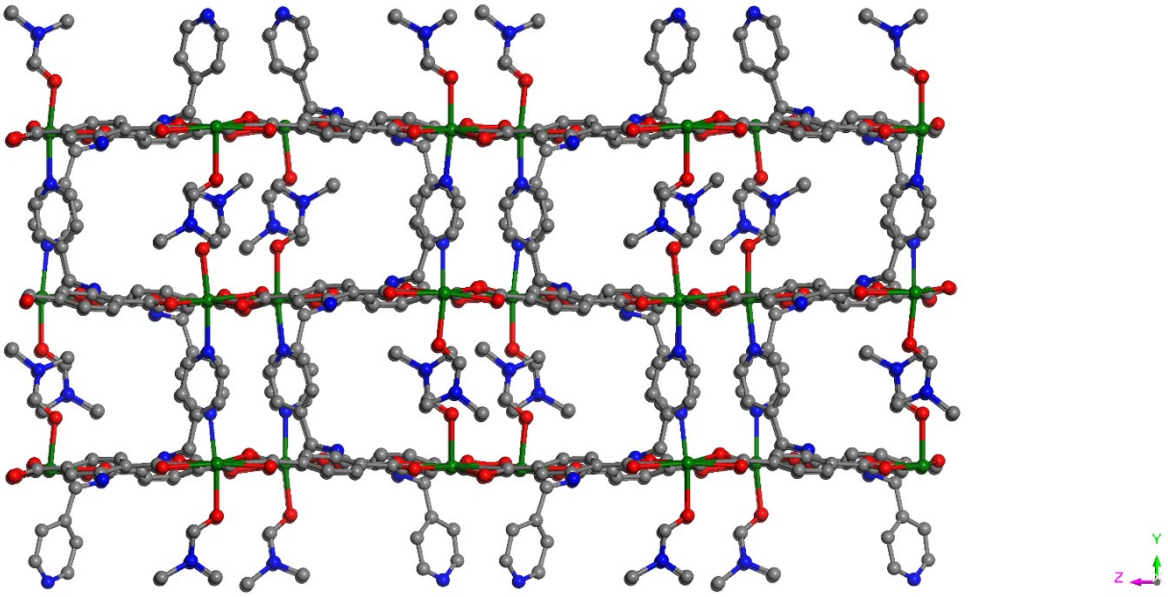

Fig. S8. Ball-and-stick representation of the 3D structure of **IITG-6**, viewed down the x-axis.

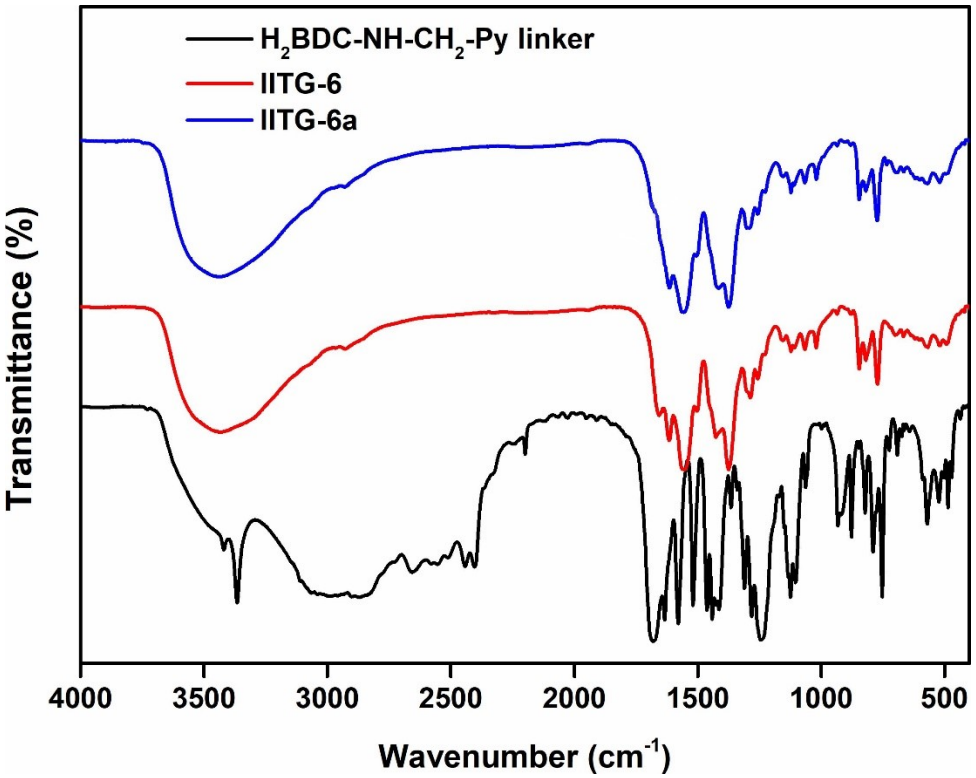

Fig. S9. FT-IR spectra of (a) H_2BDC-NH-CH_2-Py linker, (b) as-synthesized **IITG-6** and (c) activated **IITG-6a**.

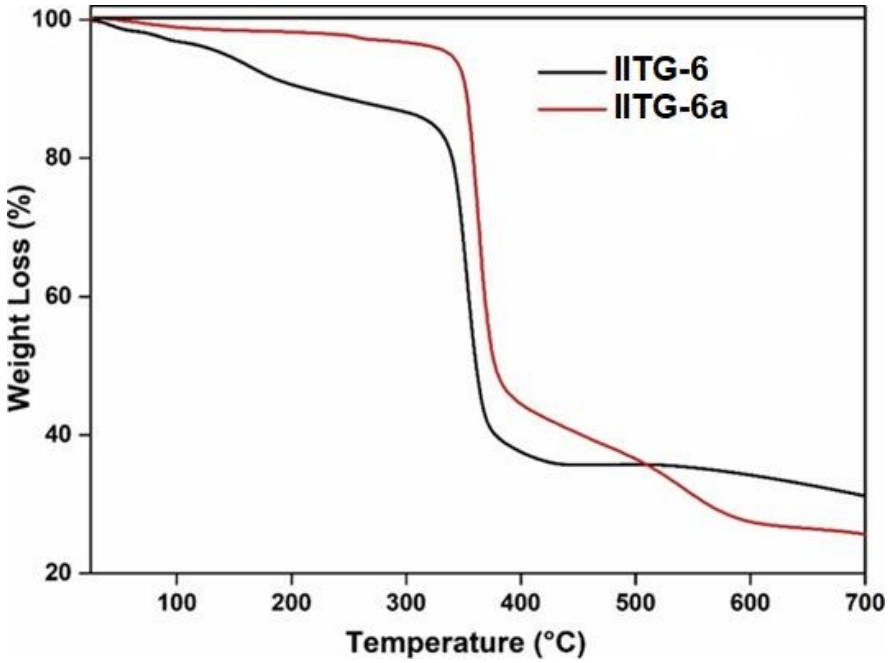

Fig. S10. TG curves of as-synthesized **IITG-6** (black) and thermally activated **IITG-6a** (red) recorded under an argon atmosphere in the temperature range of 25-700 °C with a heating rate of 10 °C min^{-1}.

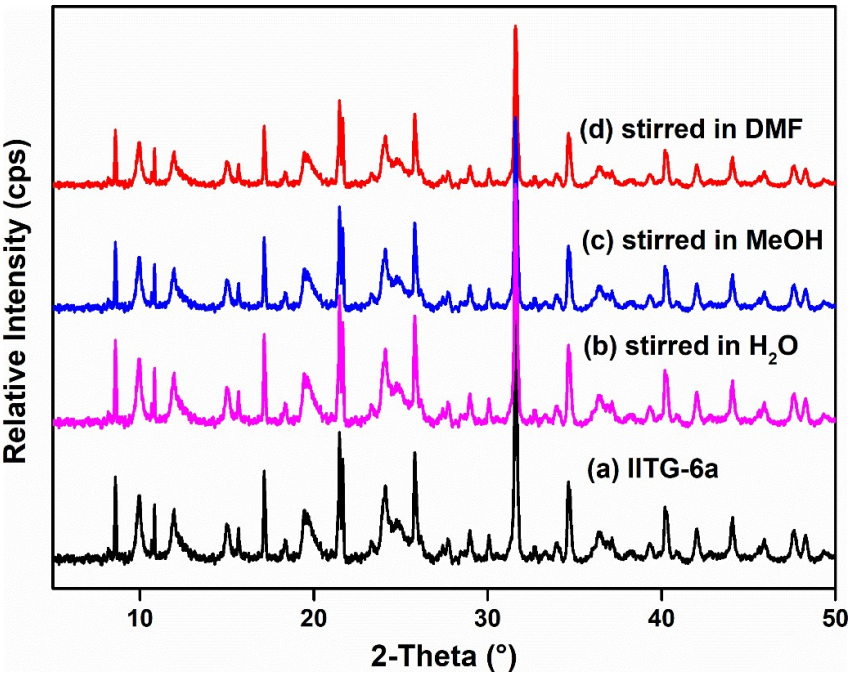

Fig. S11. XRPD patterns of **IITG-6a** after stirring in different solvents: (a) fresh **IITG-6a**, **IITG-6a** after stirring in (b) H_2O, (c) MeOH and (d) DMF for 4 h.

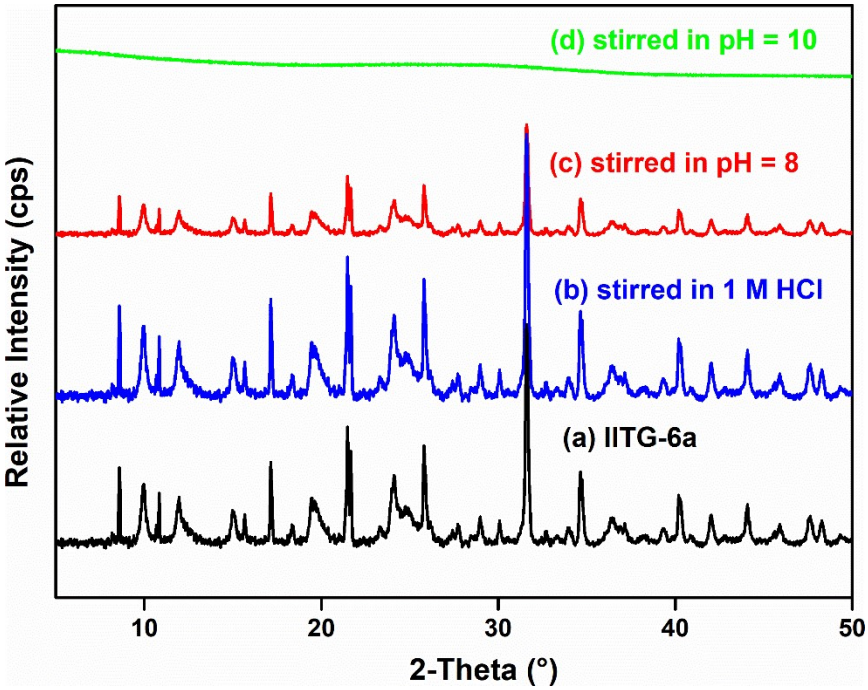

Fig. S12. XRPD patterns of **IITG-6a** after stirring in different solvents: (a) 1 M HCl, (b) pH = 8 and pH = 10 for 4 h.

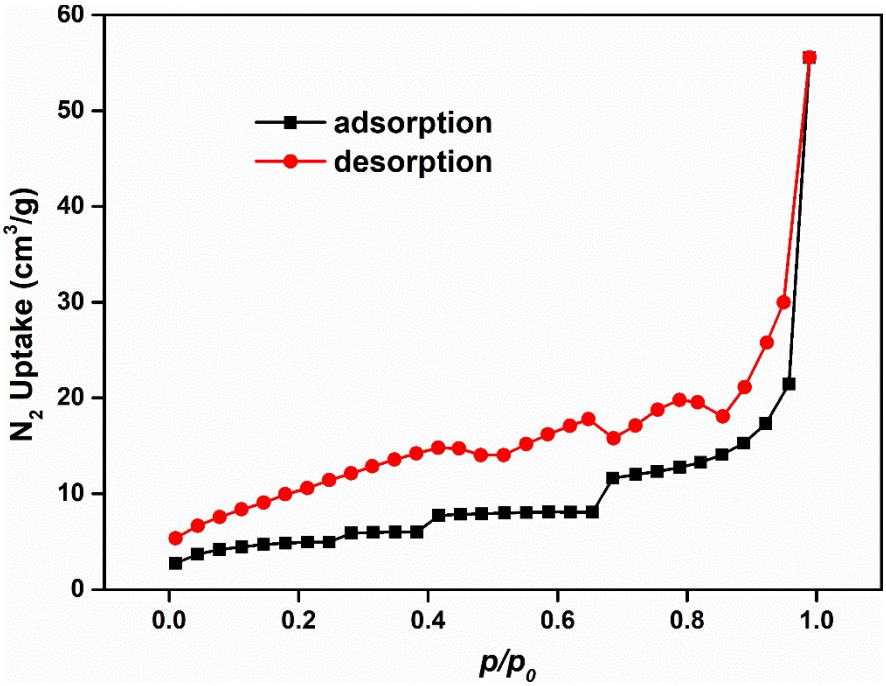

Fig. S13. N_2 adsorption (black circles) and desorption (red circles) isotherms of **IITG-6a** recorded at –196 °C.

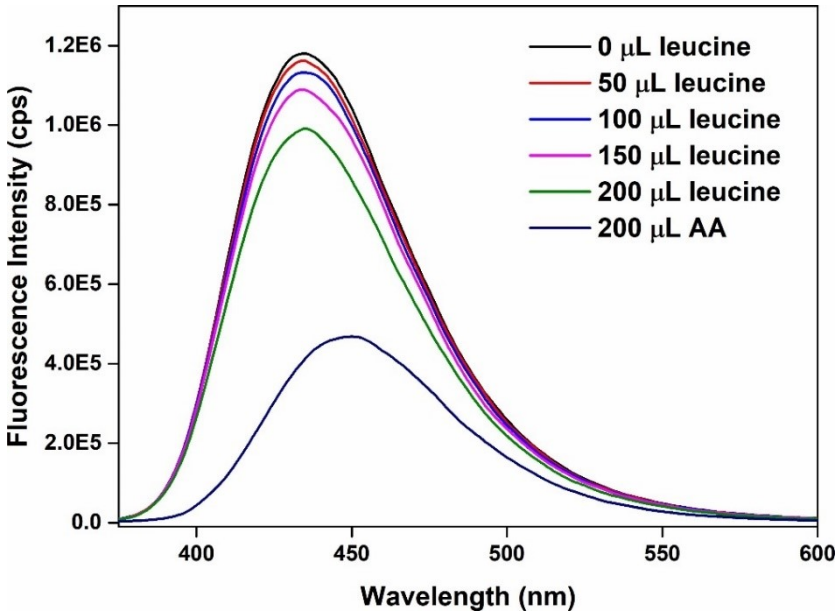

Fig. S14. Quenching of the fluorescence intensity of the suspension of **IITG-6a** (in water) upon the addition of 200 μL of 10 mM AA (Ascorbic Acid) solution in presence of 200 μL of 10 mM leucine solution in water.

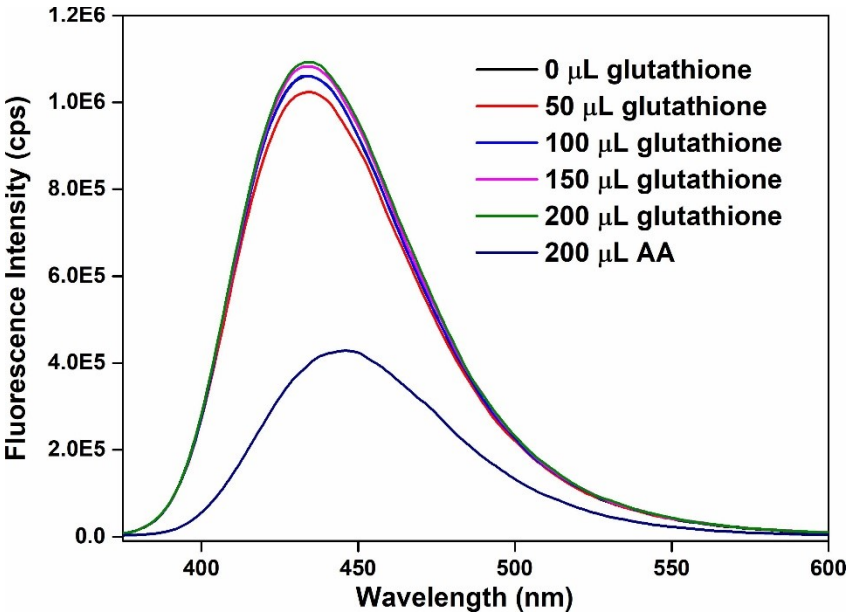

Fig. S15. Quenching of the fluorescence intensity of the suspension of **IITG-6a** (in water) upon the addition of 200 μL of 10 mM AA (Ascorbic Acid) solution in presence of 200 μL of 10 mM glutathione solution in water.

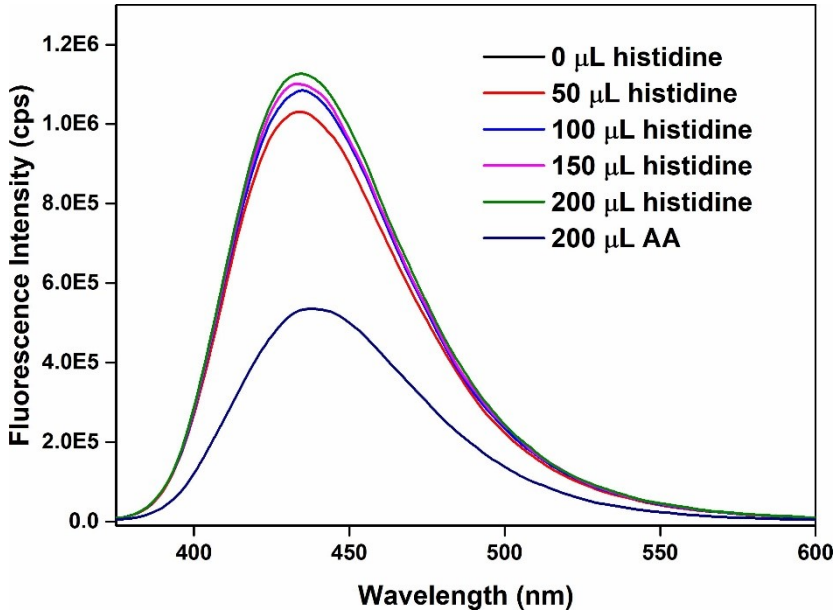

Fig. S16. Quenching of the fluorescence intensity of the suspension of **IITG-6a** (in water) upon the addition of 200 μL of 10 mM AA (Ascorbic Acid) solution in presence of 200 μL of 10 mM histidine solution in water.

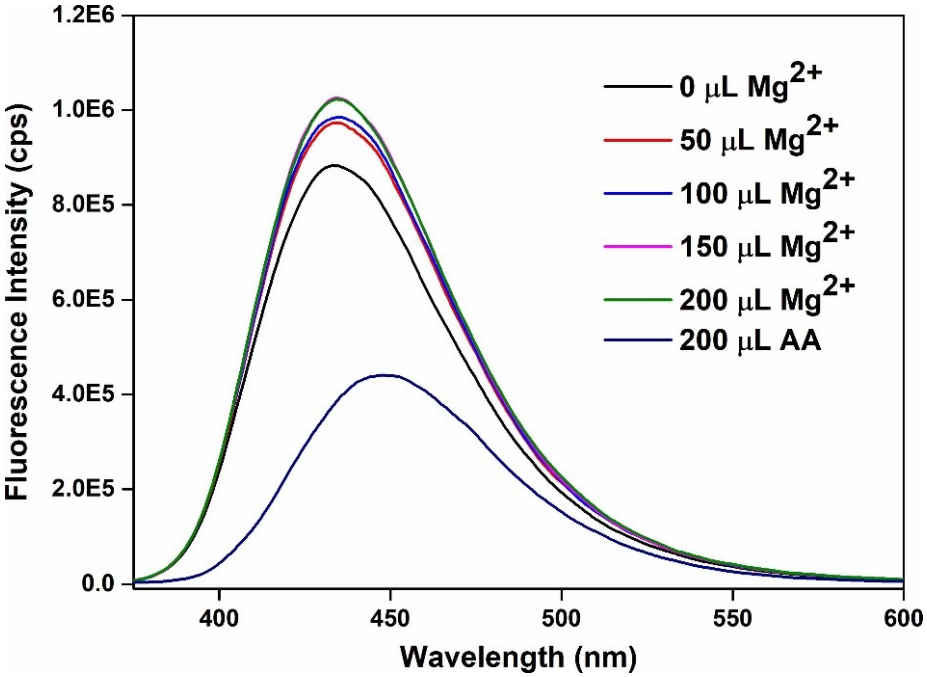

Fig. S17. Quenching of the fluorescence intensity of the suspension of **IITG-6a** (in water) upon the addition of 200 μL of 10 mM AA (Ascorbic Acid) solution in presence of 200 μL of 10 mM Mg^{2+} solution in water.

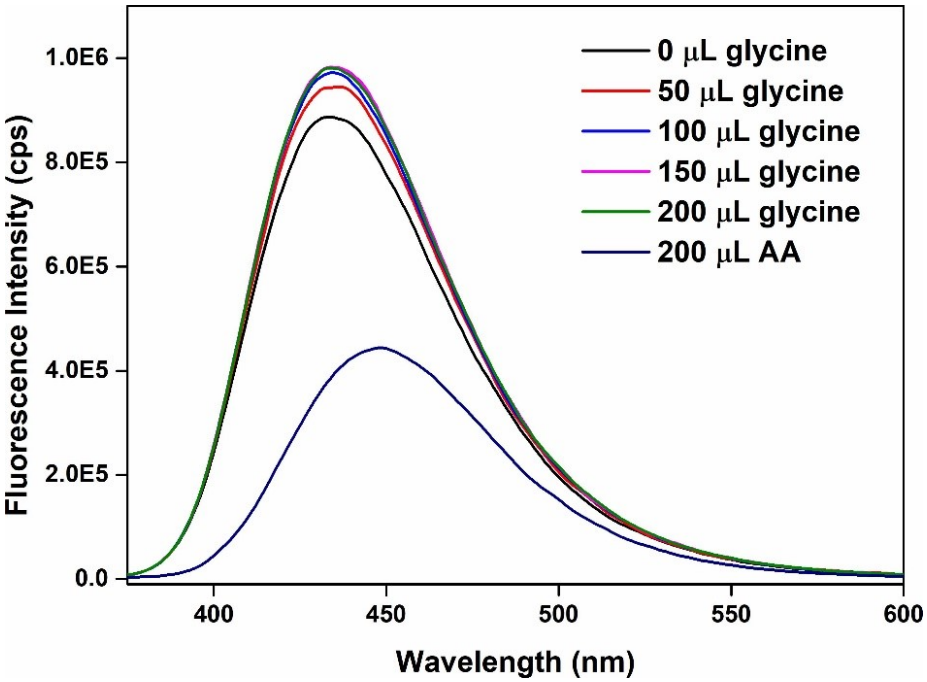

Fig. S18. Quenching of the fluorescence intensity of the suspension of **IITG-6a** (in water) upon the addition of 200 μL of 10 mM AA (Ascorbic Acid) solution in presence of 200 μL of 10 mM glycine solution in water.

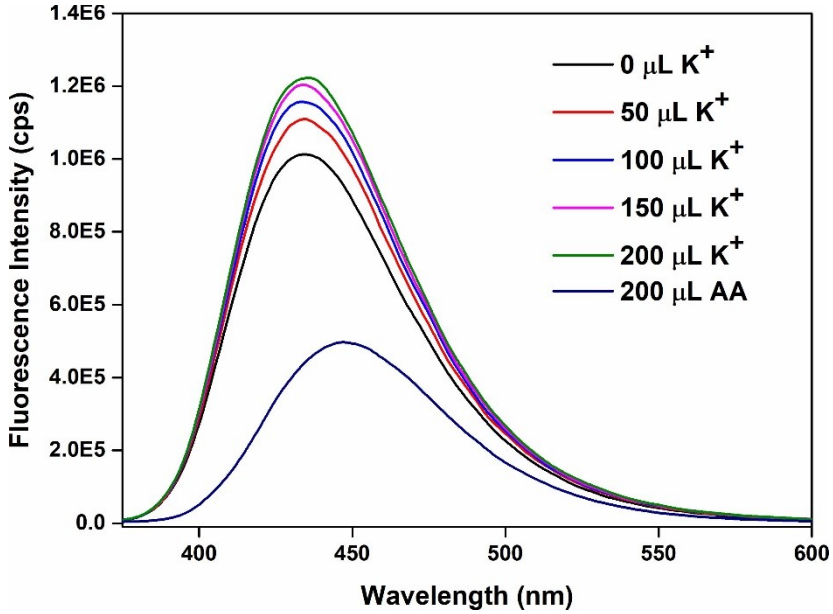

Fig. S19. Quenching of the fluorescence intensity of the suspension of **IITG-6a** (in water) upon the addition of 200 μL of 10 mM AA (Ascorbic Acid) solution in presence of 200 μL of 10 mM K^+ solution in water.

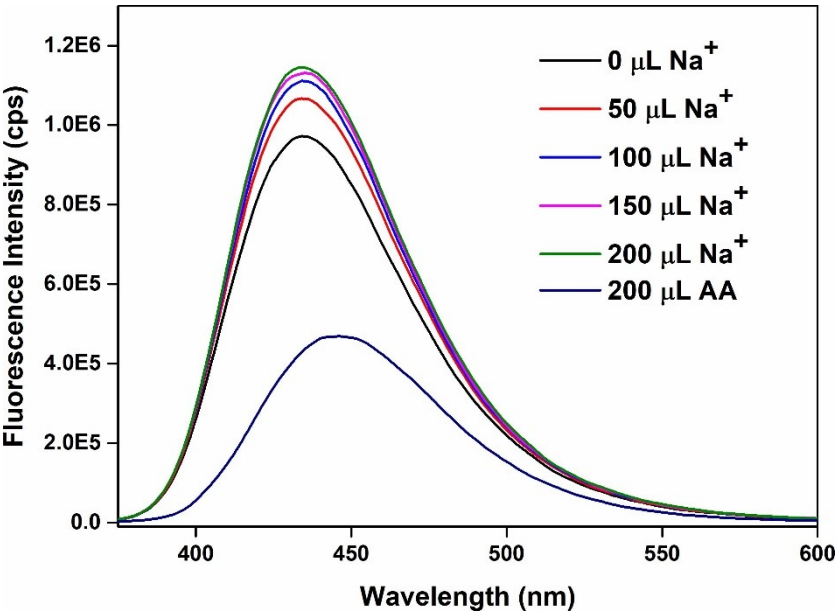

Fig. S20. Quenching of the fluorescence intensity of the suspension of **IITG-6a** (in water) upon the addition of 200 μL of 10 mM AA (Ascorbic Acid) solution in presence of 200 μL of 10 mM Na^+ solution in water.

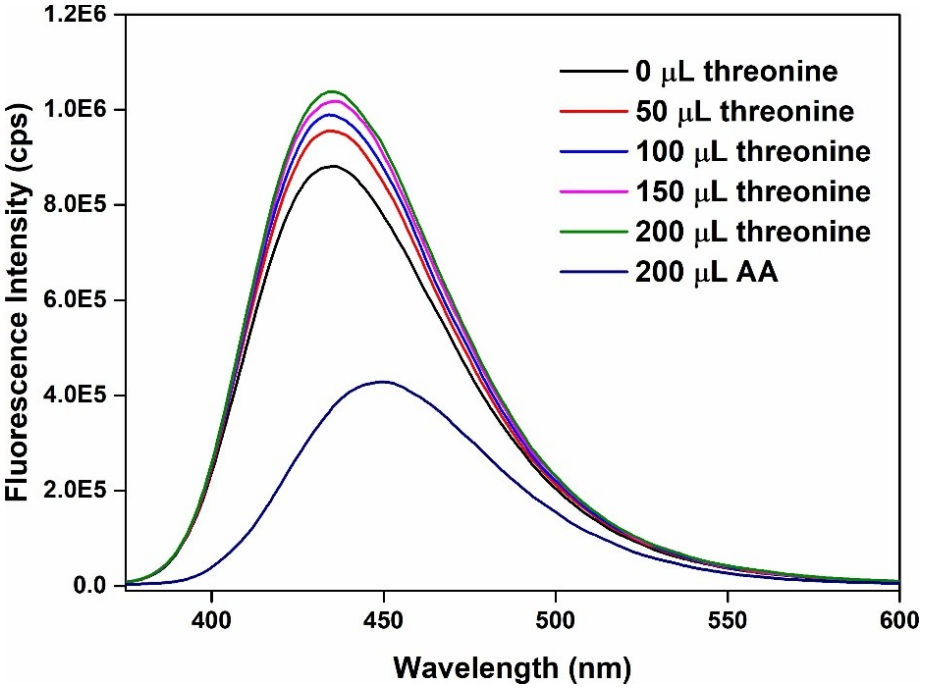

Fig. S21. Quenching of the fluorescence intensity of the suspension of **IITG-6a** (in water) upon the addition of 200 μL of 10 mM AA (Ascorbic Acid) solution in presence of 200 μL of 10 mM threonine solution in water.

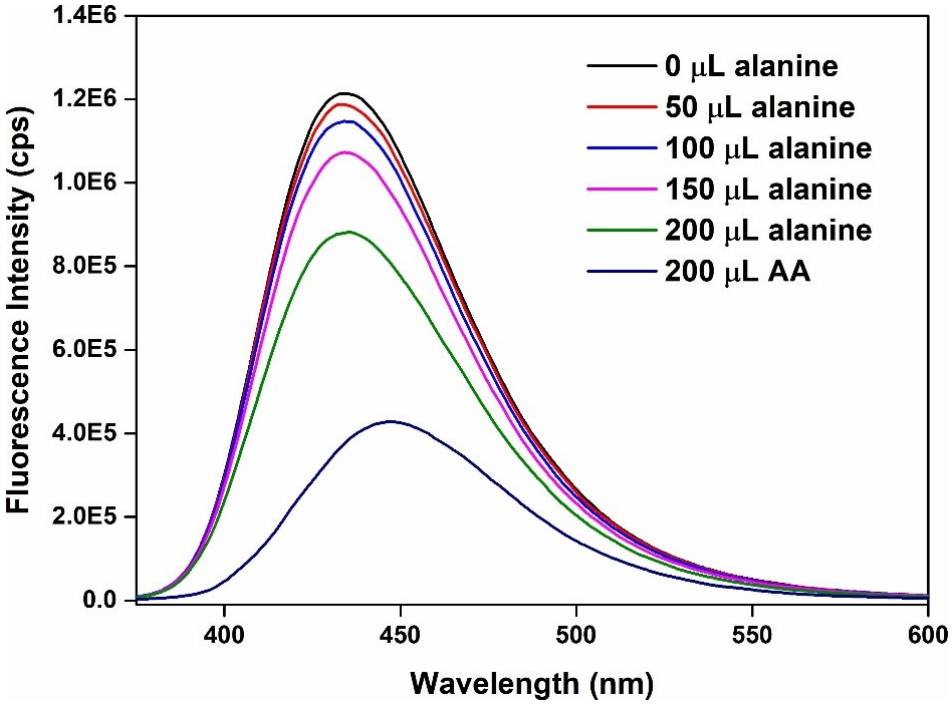

Fig. S22. Quenching of the fluorescence intensity of the suspension of **IITG-6a** (in water) upon the addition of 200 μL of 10 mM AA (Ascorbic Acid) solution in presence of 200 μL of 10 mM alanine solution in water.

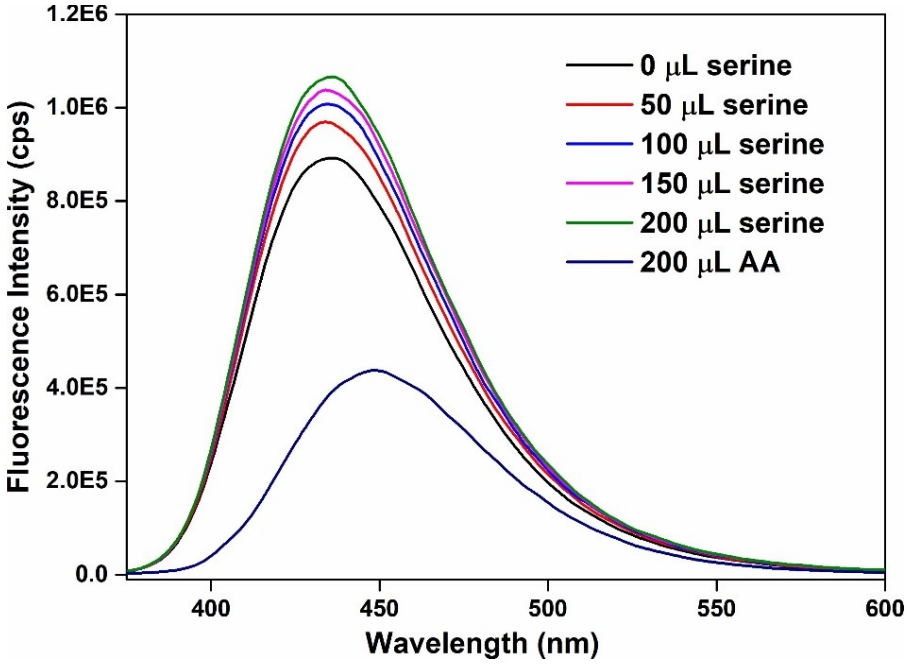

Fig. S23. Quenching of the fluorescence intensity of the suspension of **IITG-6a** (in water) upon the addition of 200 μL of 10 mM AA (Ascorbic Acid) solution in presence of 200 μL of 10 mM serine solution in water.

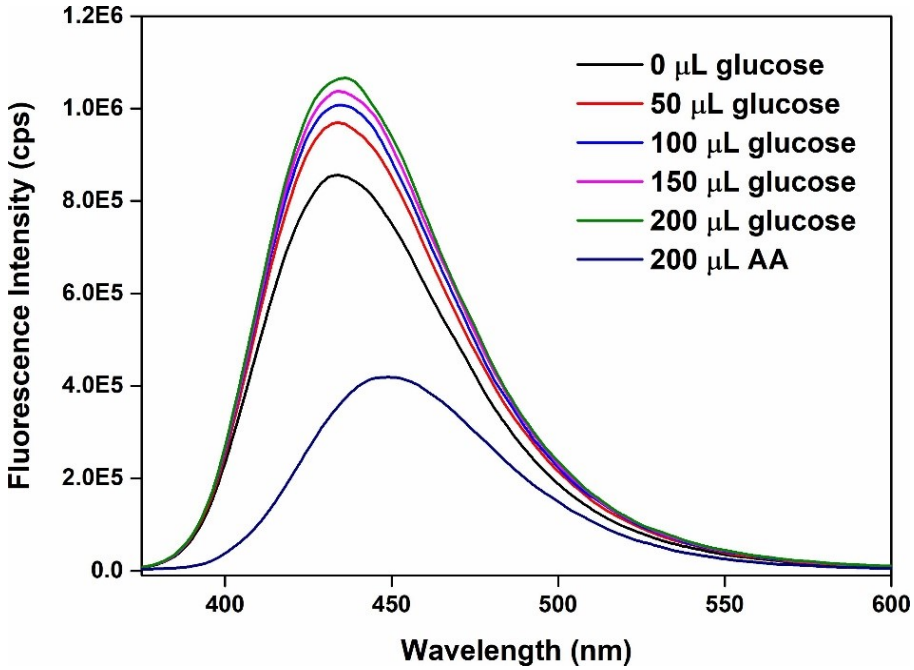

Fig. S24. Quenching of the fluorescence intensity of the suspension of **IITG-6a** (in water) upon the addition of 200 μL of 10 mM AA (Ascorbic Acid) solution in presence of 200 μL of 10 mM glucose solution in water.

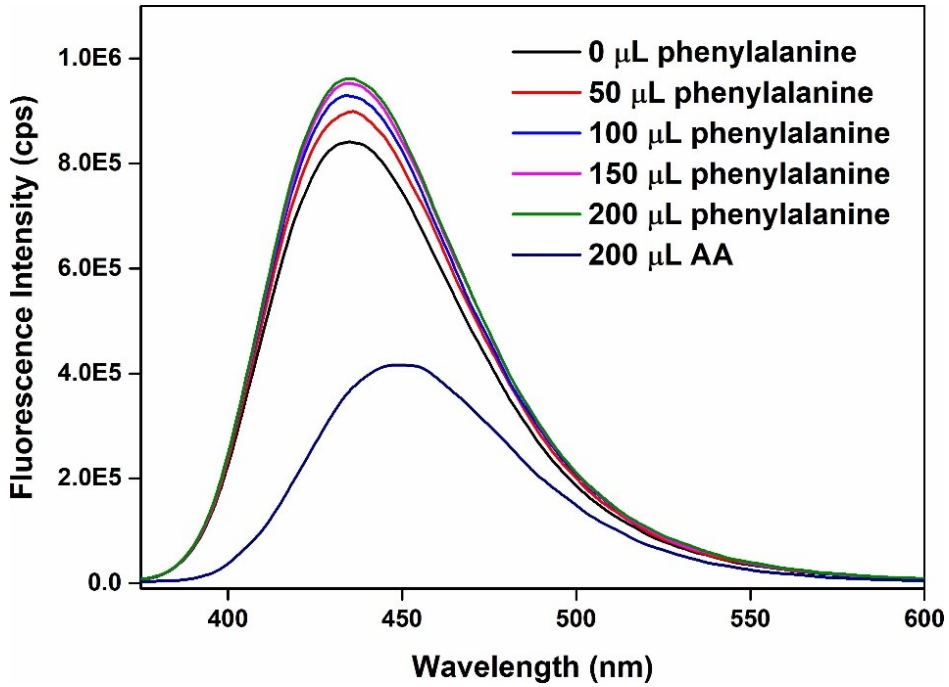

Fig. S25. Quenching of the fluorescence intensity of the suspension of **IITG-6a** (in water) upon the addition of 200 μL of 10 mM AA (Ascorbic Acid) solution in presence of 200 μL of 10 mM phenylalanine solution in water.

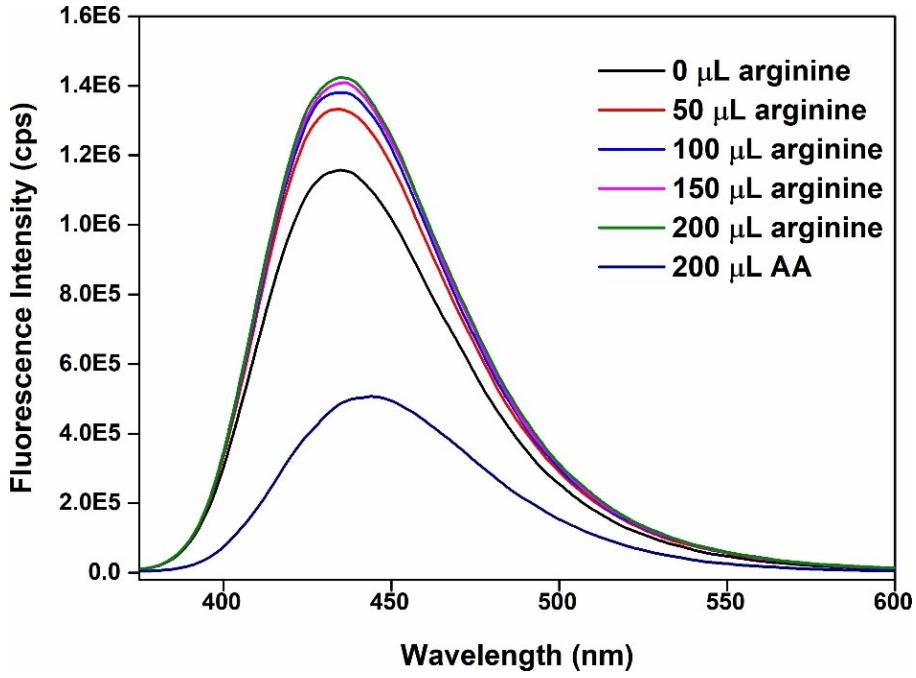

Fig. S26. Quenching of the fluorescence intensity of the suspension of **IITG-6a** (in water) upon the addition of 200 μL of 10 mM AA (Ascorbic Acid) solution in presence of 200 μL of 10 mM arginine solution in water.

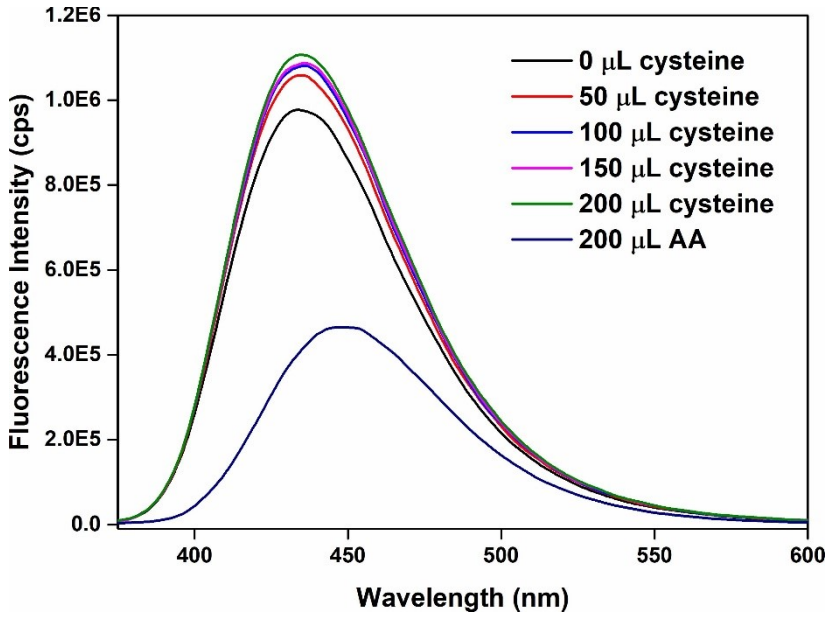

Fig. S27. Quenching of the fluorescence intensity of the suspension of **IITG-6a** (in water) upon the addition of 200 μL of 10 mM AA (Ascorbic Acid) solution in presence of 200 μL of 10 mM cysteine solution in water.

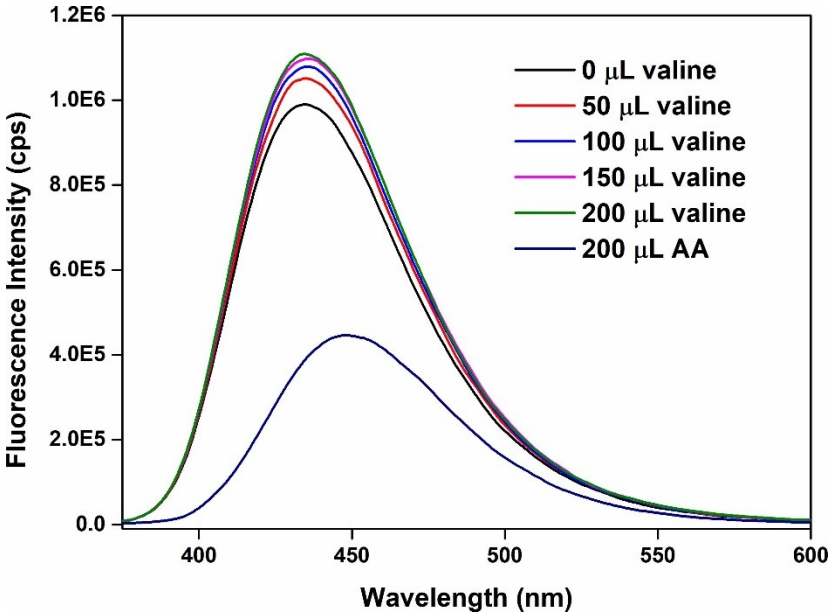

Fig. S28. Quenching of the fluorescence intensity of the suspension of **IITG-6a** (in water) upon the addition of 200 μL of 10 mM AA (Ascorbic Acid) solution in presence of 200 μL of 10 mM valine solution in water.

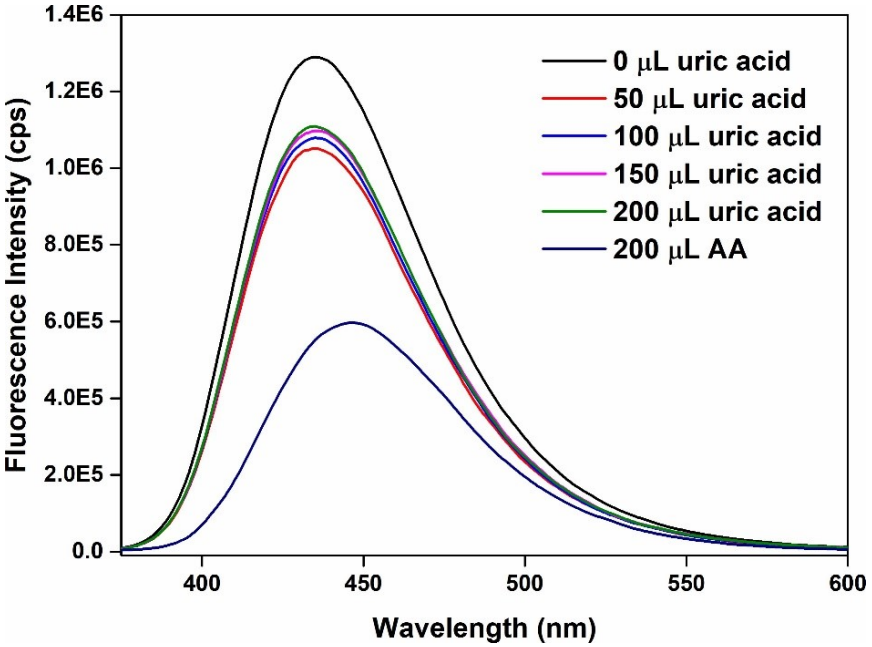

Fig. S29. Quenching of the fluorescence intensity of the suspension of **IITG-6a** (in water) upon the addition of 200 μL of 10 mM AA (Ascorbic Acid) solution in presence of 200 μL of 10 mM uric acid solution in water.

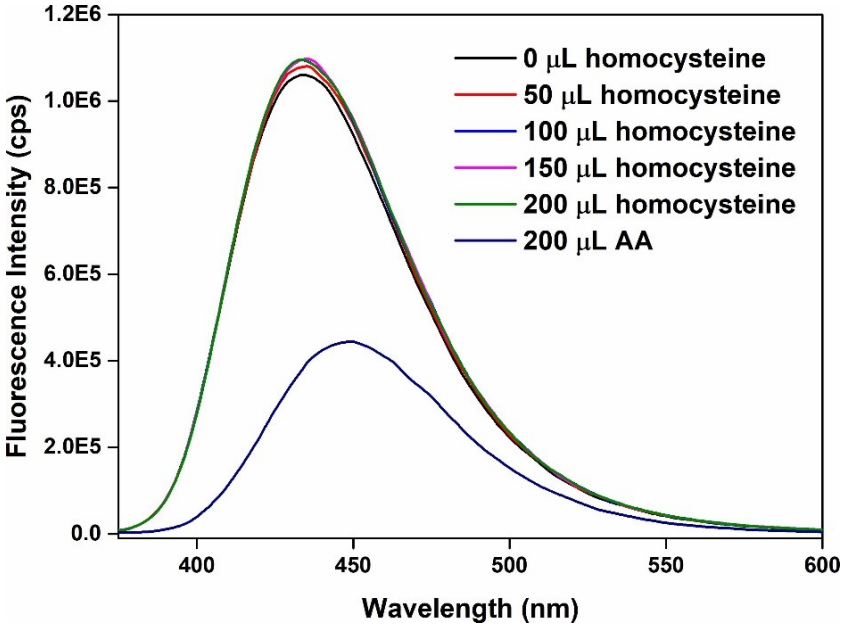

Fig. S30. Quenching of the fluorescence intensity of the suspension of **IITG-6a** (in water) upon the addition of 200 μL of 10 mM AA (Ascorbic Acid) solution in presence of 200 μL of 10 mM homocysteine solution in water.

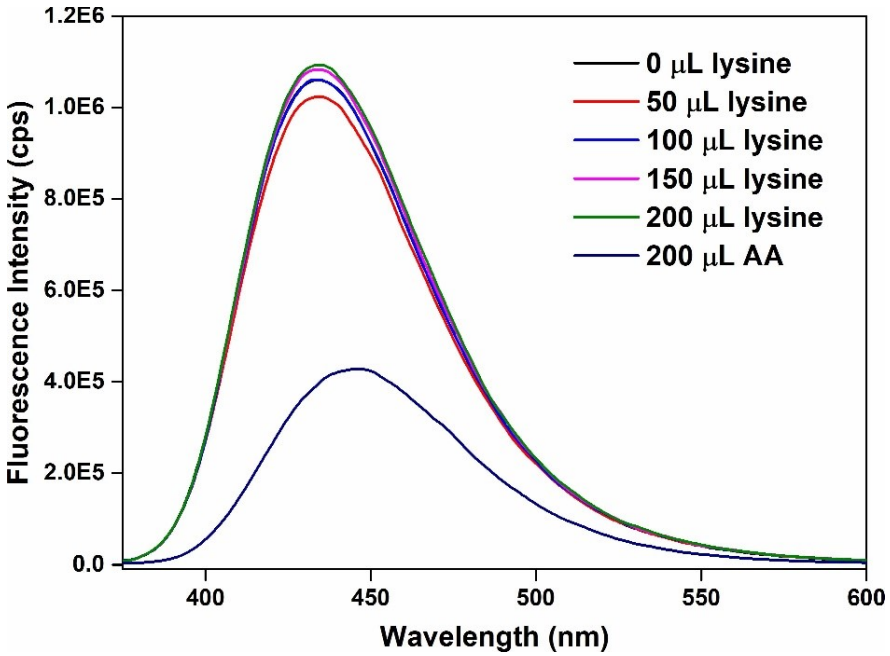

Fig. S31. Quenching of the fluorescence intensity of the suspension of **IITG-6a** (in water) upon the addition of 200 μL of 10 mM AA (Ascorbic Acid) solution in presence of 200 μL of 10 mM lysine solution in water.

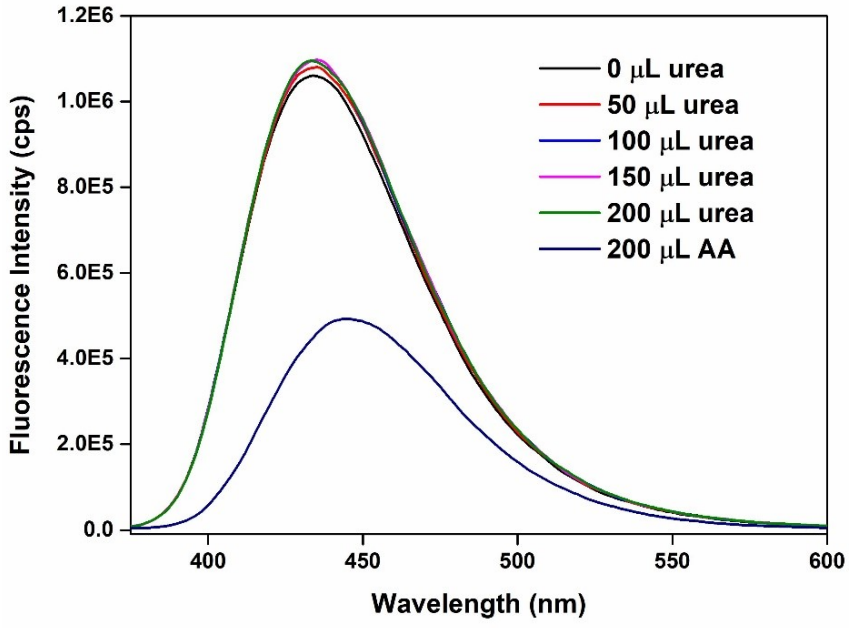

Fig. S32. Quenching of the fluorescence intensity of the suspension of **IITG-6a** (in water) upon the addition of 200 μL of 10 mM AA (Ascorbic Acid) solution in presence of 200 μL of 10 mM urea solution in water.

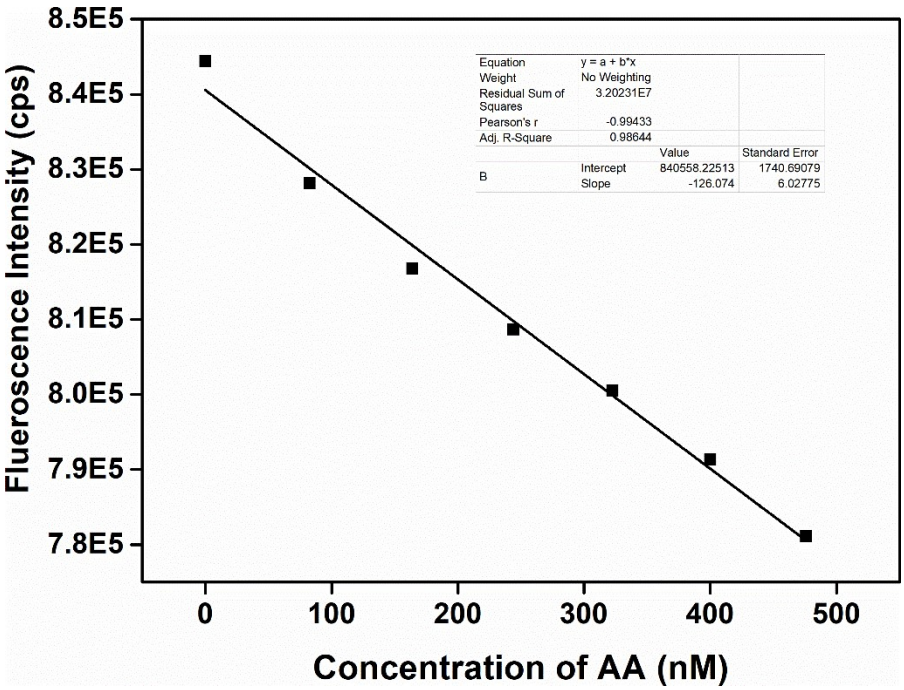

Fig. S33. Change in the fluorescence intensity of **IITG-6a** in water as a function of AA concentration.

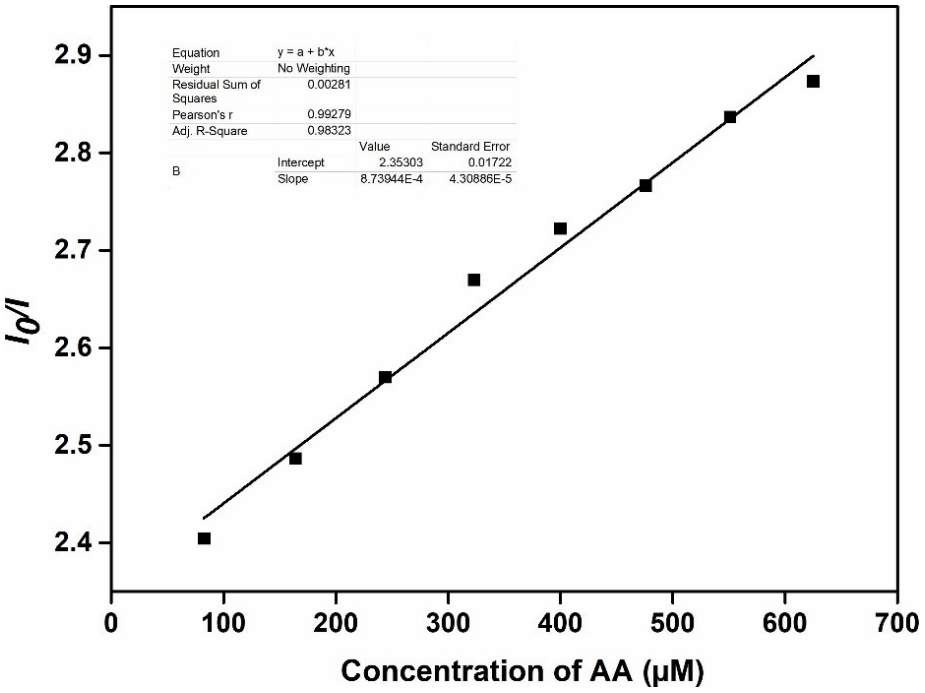

Fig. S34. Stern-Volmer plot for the fluorescence quenching of **IITG-6a** in water upon addition of AA.

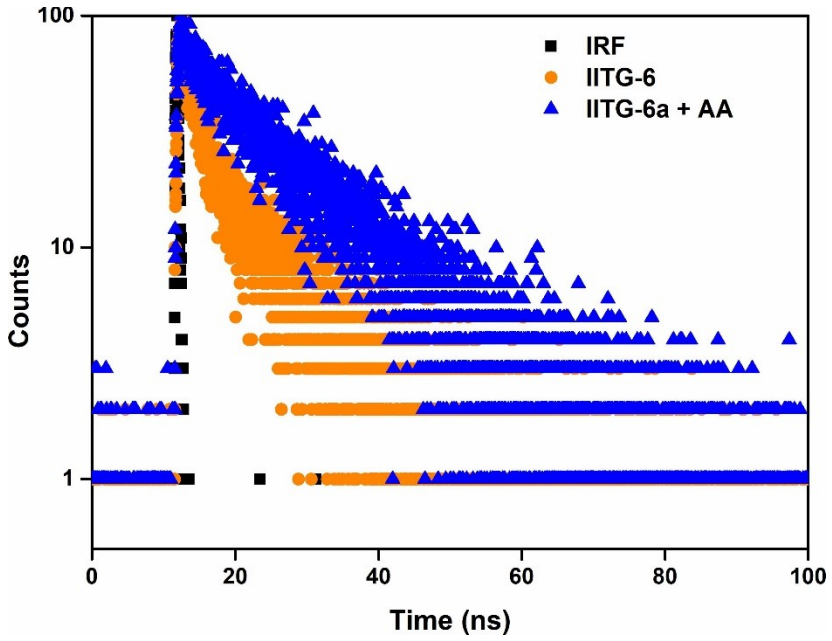

Fig. S35. Lifetime decay profile of **IITG-6a** before and after the addition of 125 µL of 10 mM AA in water.

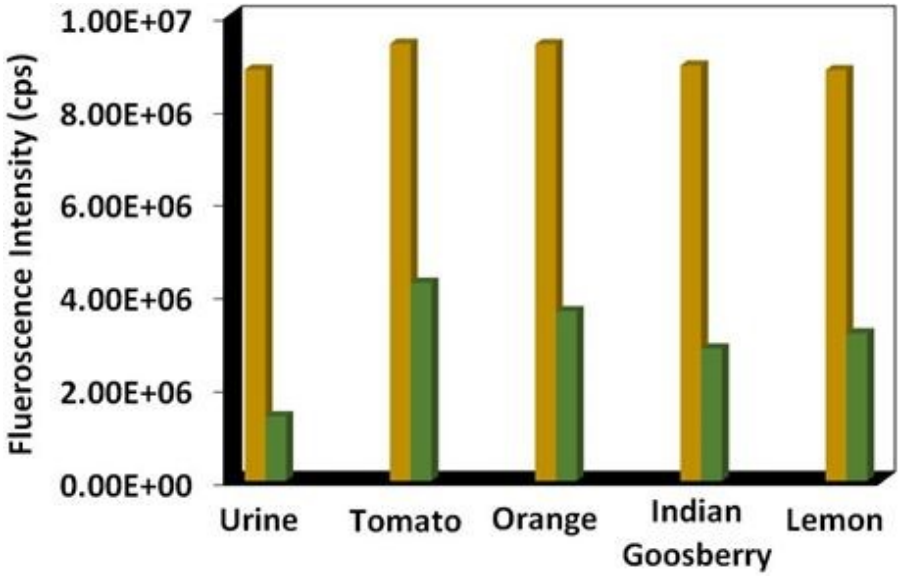

Fig. S36. Fluorescence response of **IITG-6a** towards AA present in human urine, orange juice, Indian gooseberry and lemon juice (grey color bars represent the fluorescence intensities of **IITG-6a** before the addition of various real samples and the green color bars represents the fluorescence intensities of **IITG-6a** after the addition of various real samples).

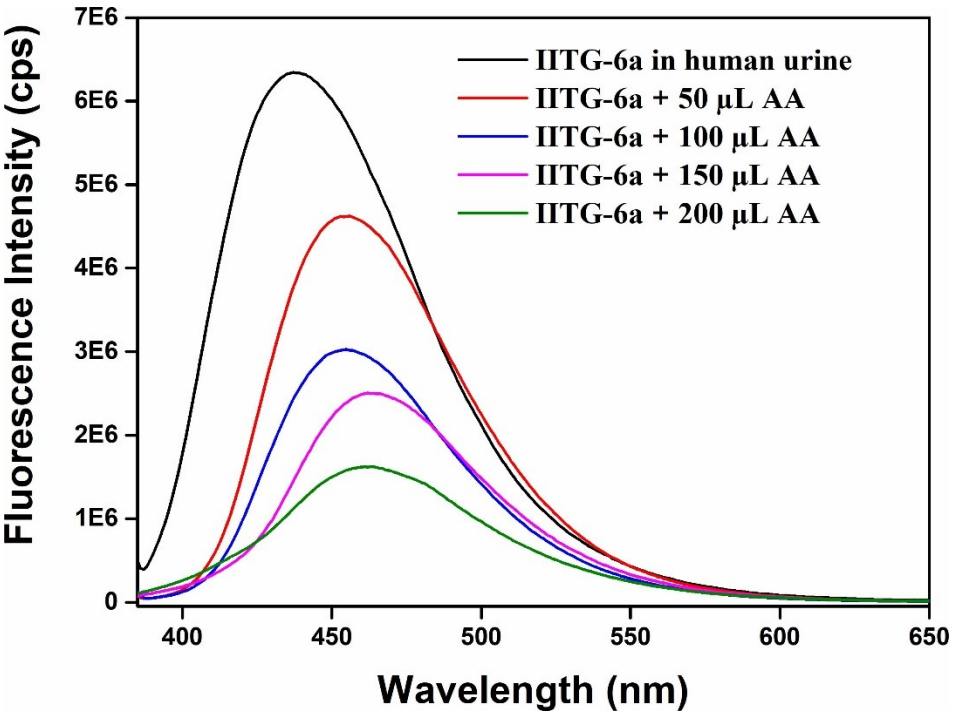

Fig. S37. Quenching of the fluorescence intensity of the suspension of **IITG-6a** (in human urine) upon the addition of 200 µL of 10 mM AA (Ascorbic Acid) solution.

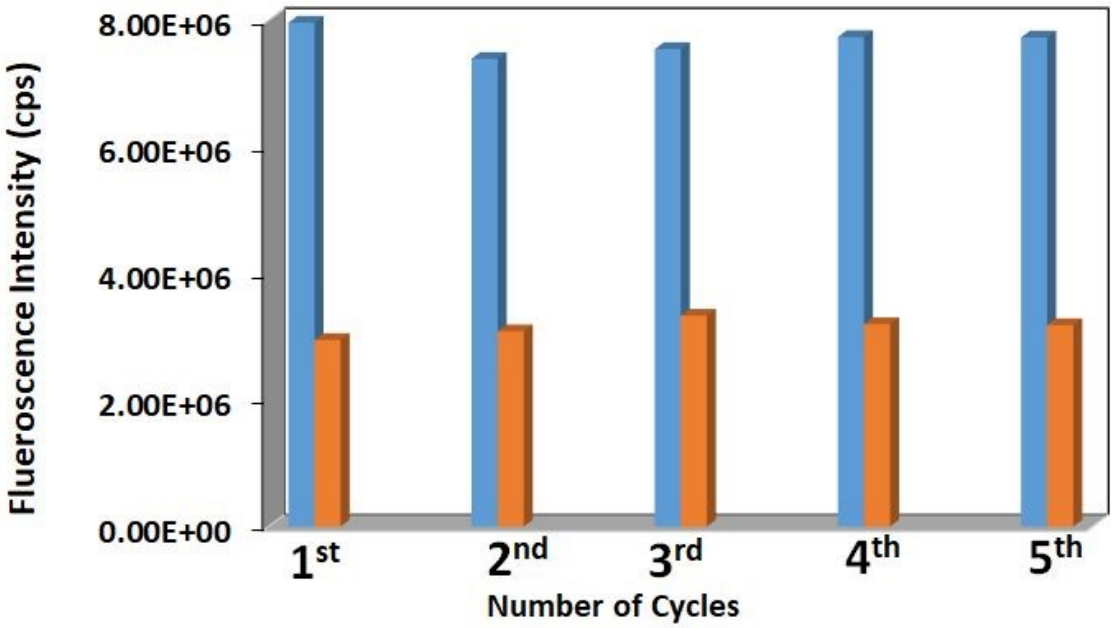

Fig. S38. Recyclability test for the fluorescence turn-off response of the suspension of **IITG-6a** towards 10 mM AA solution in water (blue color bars represent the fluorescence intensities of **IITG-6a** before the addition of AA and the saffron color bars represents the fluorescence intensities of **IITG-6a** after the addition of AA).

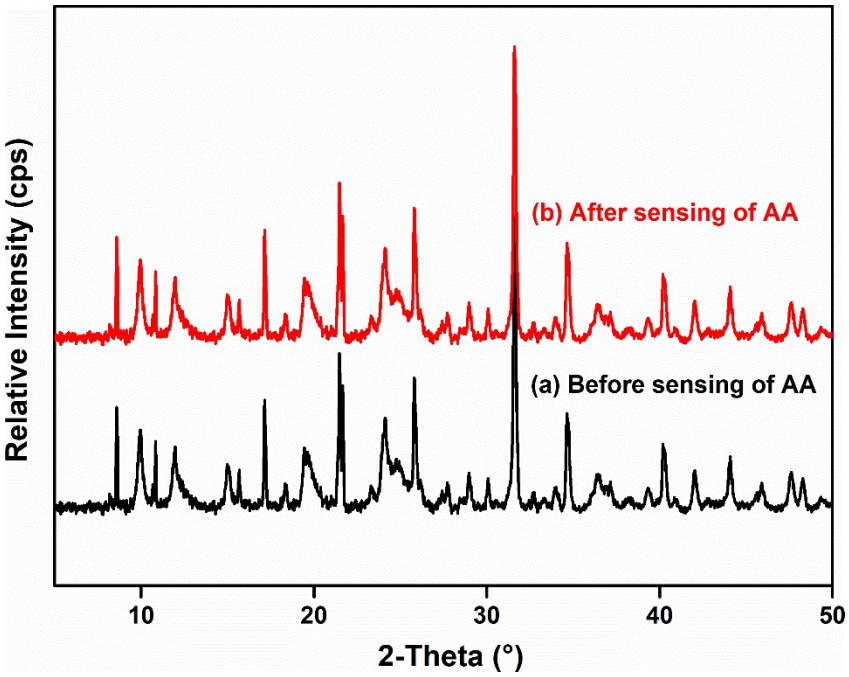

Fig. S39. XRPD pattern of **IITG-6a** (a) before and (b) after the addition of 200 µL of 10 mM AA in water.

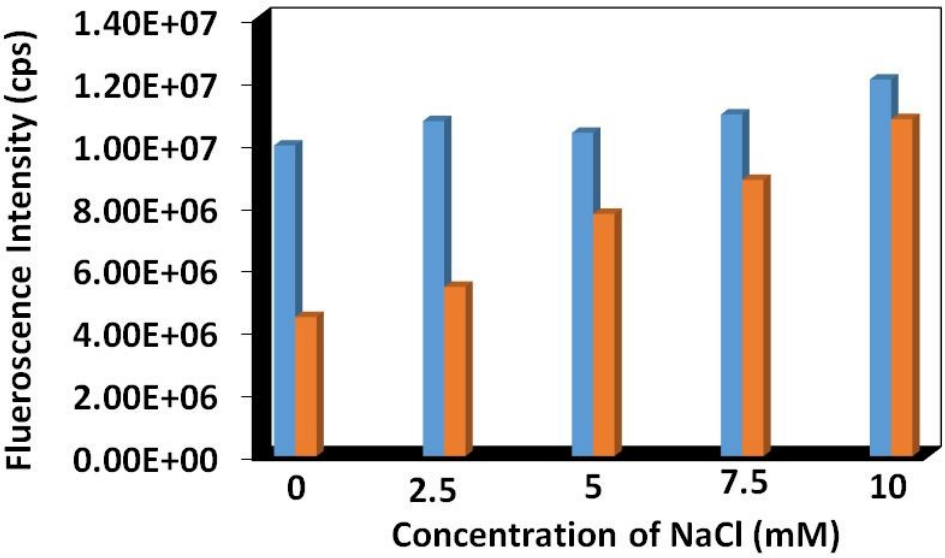

Fig. S40. Salt-induced (NaCl) screening of the extent of interaction of **IITG-6a** MOF with AA in water (λ_{ex} = 350 nm and λ_{em} = 448 nm) (blue color bars represent the fluorescence intensities of **IITG-6a** before the addition of AA and the saffron color bars represents the fluorescence intensities of **IITG-6a** after the addition of AA).

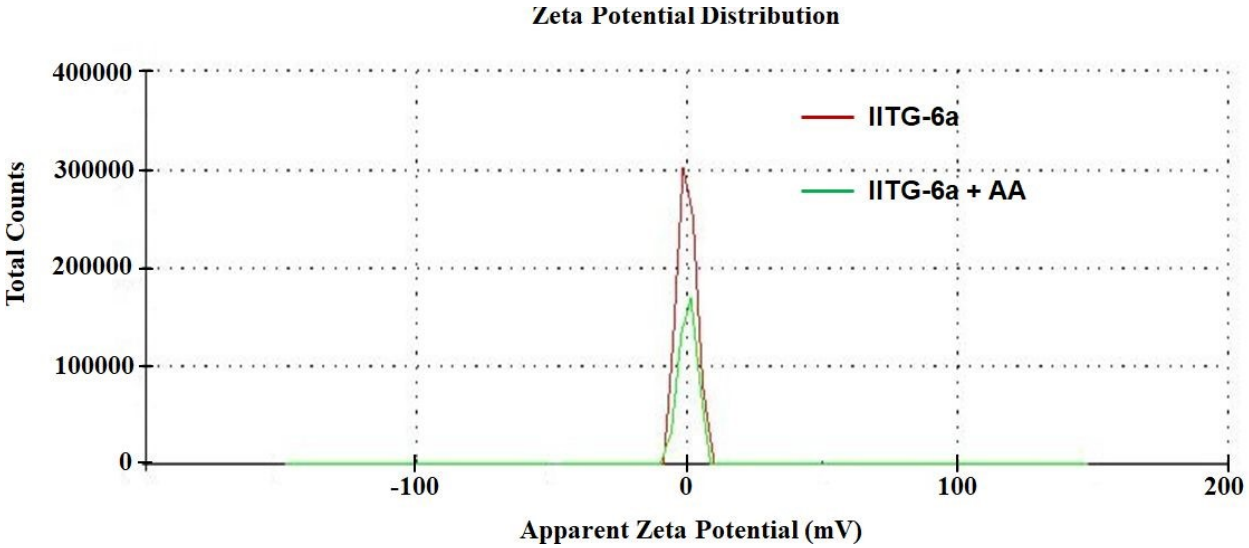

Fig. S41. Zeta potential distribution of **IITG-6a** in water before and after addition of AA.

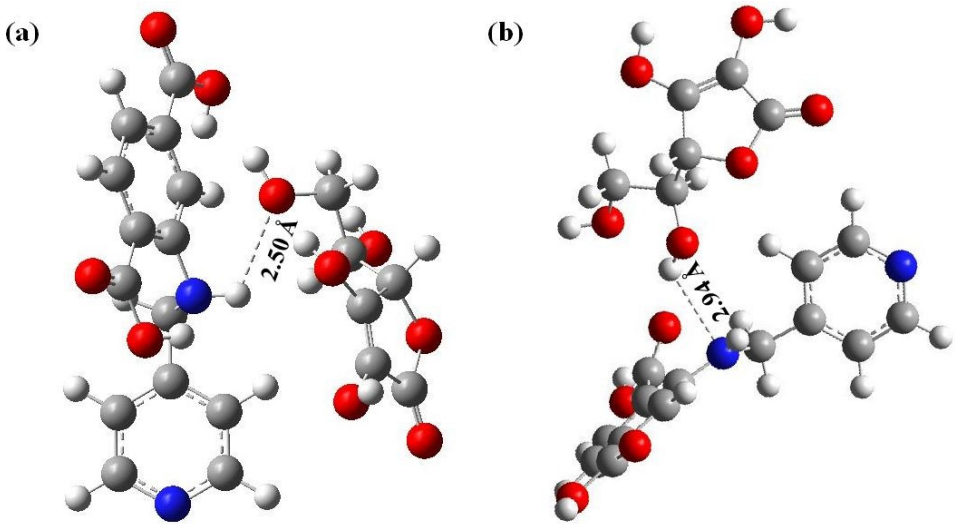

Fig. S42. (a) Original H-bonding between $–CH_2$-OH group of the AA and –NH- group of the linker molecule and (b) other possible H-bonding between –CH-OH group of AA and –NH of the linker molecule.

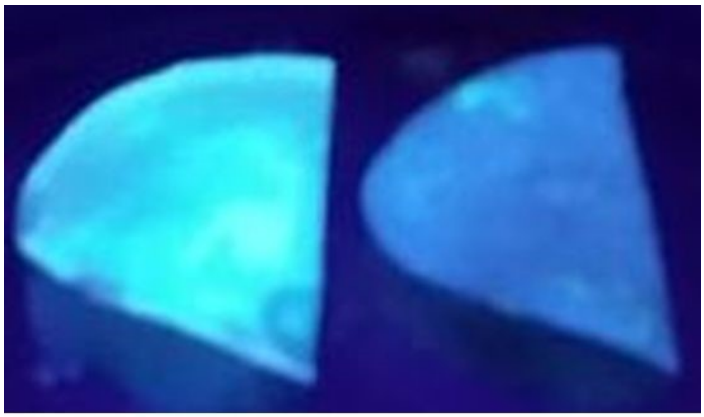

Fig. S43. Images of **IITG-6a**-coated paper strips under UV lamp after and before the treatment of 10 mM aqueous AA solution.

Table S1. Crystallographic Parameters for the Crystal Structure of **IITG-6**.

Compound	**IITG-6**
Formula unit	$C_{34}H_{32}Cd_2N_6O_{10}$
Formula weight ($gmol^{-1}$)	909.48
T (K)	100
Crystal system	orthorhombic
Space group	$P2_12_12_1$
a (Å)	13.3653(2)
b (Å)	14.7692(2)
c (Å)	20.6731(3)
α (°)	90
β (°)	90
γ (°)	90
V ($Å^3$)	4080.76(10)
Z	4
ρ_{calc} (gcm^{-3})	1.480
$2\theta_{max}$ (°)	59.44
$F(000)$	1816
Measured reflections	45999
Unique reflections	10230
Observed reflections ($I > 2\sigma(I)$)	9092
Parameters refined	474

R_1	0.0342
wR_2	0.0816
R_1 (all data)	0.0410
wR_2 (all data)	0.0852
Goodness-of-fit (GOF)	1.041
μ (mm^{-1})	1.099
CCDC-entry	1937854

Table S2. Average excited-state lifetime (<τ >*) values of **IITG-6a** before and after the addition of 200 μL of 10 mM AA solution in water.

Volume of AA solution added (μL)	a_1	a_2	τ_1 (ns)	τ_2 (ns)	<τ >* (ns)
0	0.05	0.95	2.65	14.32	13.74
200	0.35	0.65	2.06	12.52	8.86

Table S3. Comparison of the response time, detection limit and sensing media used for the reported chemosensors of AA in the literature.

Sl. No.	Sensor Material	Type of Material	Sensing Medium	Detection Limit (nM)	Response Time (s)	Detection method	Ref
1	$[Cd(C_{14}H_{10}N_2O_4)(C_3H_7NO)]\cdot 1.5H_2O0.5C_3H_7NO$	MOF	Water	31	< 60	Fluorescence	This work
2	MOF-5/3D-KSC	MOF	PBS	240	-	Electrochemical	5
3	$Eu_{0.07}Gd_{0.03}$-MOF	MOF	Water	184	-	Ratiometric	6
4	Im@Eu-MOF	MOF	Water	100	-	Fluorescence	7
5	CuNPs@C	Nanoparticles	Water	141	-	Fluorescence	8
6	RhB@ $DiCH_3$MOF-5	MOF	Water	310	310	Fluorescence	9
7	ZJU-137	MOF	Water	34	-	Fluorescence	10
8	Ce-MOF	MOF	Water-DMF	30	300	Colorimetric	11

9	Au NCs	nanocrystals	Water	200	300	Fluorescence	12
10	CQDs-MnO_2	CQDs	Water	42	180	Fluorescence	13

Table S4. Bond distances of the Cd atoms of **IITG-6** compound.

Atom	**Atom**	**Length/Å**
Cd1	O1	2.403(3)
Cd1	O5[1]	2.383(3)
Cd1	O6[1]	2.431(3)
Cd1	O7[2]	2.341(3)
Cd1	O8[2]	2.429(3)
Cd1	O10	2.268(3)
Cd1	N4	2.306(4)
Cd1	C22[2]	2.726(4)
Cd2	O1[3]	2.349(3)
Cd2	O2[3]	2.435(3)
Cd2	O3[4]	2.443(3)
Cd2	O4[4]	2.330(3)
Cd2	O5	2.403(3)
Cd2	O9	2.301(3)
Cd2	N2	2.322(4)
Cd2	C1[3]	2.749(4)
Cd2	C8[4]	2.730(4)

[1]1/2+X,3/2-Y,1-Z; [2]2-X,-1/2+Y,1/2-Z; [3]-1/2+X,3/2-Y,1-Z; [4]1-X,1/2+Y,1/2-Z

Table S5. Bond angles of the Cd atoms of **IITG-6** compound.

Atom	Atom	Atom	Angle (°)
O1	Cd1	O82	97.36(9)
$O5_1$	Cd1	O1	72.54(9)
$O5_1$	Cd1	O61	54.20(9)
$O7_2$	Cd1	O61	81.65(11)
$O7_2$	Cd1	O82	54.98(10)

[1]1/2+X,3/2-Y,1-Z; [2]2-X,-1/2+Y,1/2-Z; [3]-1/2+X,3/2-Y,1-Z; [4]1-X,1/2+Y,1/2-Z; [5]1-X,-1/2+Y,1/2-Z; [6]2-X,1/2+Y,1/2-Z

References:

1. Rigaku Oxford Diffraction, (2019), CrysAlisPro Software system, version 1.171.40.53, Rigaku Corporation, Oxford, UK.
2. Dolomanov, O. V.; Bourhis, L. J.; Gildea, R. J.; Howard, J. A. K.; Puschmann, H. OLEX2: a complete structure solution, refinement and analysis program. *J. Appl. Crystallogr.* **2009,** 42, 339−341.
3. Sheldrick, G. M. SHELXT – Integrated space group and crystal structure determination. *Acta Crystallogr; Sect. A: Found. Crystallogr.* **2015,** 71, 3−8.
4. Sheldrick, G. M. Crystal structure refinement with SHELXL. *Acta Crystallogr., Sect. C: Struct. Chem* **2015,** 71, 3−8.
5. Song, Y.; Gong, C.; Su, D.; Shen, Y.; Song, Y.; Wang, L. A novel ascorbic acid electrochemical sensor based on spherical MOF-5 arrayed on a three-dimensional porous carbon electrode. *Anal. Methods* **2016,** 8, 2290-2296.
6. Yu, H.; Liu, Q.; Li, J.; Su, Z.-M.; Li, X.; Wang, X.; Sun, J.; Zhou, C.; Hu, X. A dual-emitting mixed-lanthanide MOF with high water-stability for ratiometric fluorescence sensing of Fe^{3+} and ascorbic acid. *J. Mater. Chem. C* **2021,** 9, 562-568.
7. Zhou, S.-F.; Hao, B.-B.; Lin, T.; Zhang, C.-X.; Wang, Q.-L. A dual-functional MOF for high proton conduction and sensitive detection of ascorbic acid. *Dalton Trans.* **2020,** 49, 14490-14496.
8. Tan, H.; Ma, C.; Gao, L.; Li, Q.; Song, Y.; Xu, F.; Wang, T.; Wang, L. Metal–Organic Framework-Derived Copper Nanoparticle@Carbon Nanocomposites as Peroxidase Mimics for Colorimetric Sensing of Ascorbic Acid. *Chem. Eur. J.* **2014,** 20, 16377-16383.
9. Guo, L.; Liu, Y.; Kong, R.; Chen, G.; Liu, Z.; Qu, F.; Xia, L.; Tan, W. A Metal−Organic Framework as Selectivity Regulator for Fe3+ and Ascorbic Acid Detection. *Anal. Chem.* **2019,** 91, 12453−12460.
10. Yue, D.; Huang, Y.; Zhang, J.; Zhang, X.; Cui, Y.; Yang, Y.; Qian, G. A Two-Dimensional Metal–Organic Framework as a Fluorescent Probe for Ascorbic Acid Sensing. *Eur. J. Inorg. Chem.* **2018,** 2018, 173–177.
11. Xu, D.; Qi, S.; Chen, Y.; Yin, M.; Zhang, L.; Ge, K.; X.Wei; Tian, X.; Wang, P.; Li, M.; Wei, J.; Wang, Z.; Qiu, J. Hierarchical mesoporous hollow Ce-MOF nanosphere as oxidase

mimic for highly sensitive colorimetric detection of ascorbic acid. *Chem. Phys. Lett.* **2021,** 777, 138749-138754.
12. Liu, J.; Chen, Y.; Wang, W.; Feng, J.; Liang, M.; Ma, S.; Chen, X. "Switch-On" Fluorescent Sensing of Ascorbic Acid in Food Samples Based on Carbon Quantum Dots–MnO_2 Probe. *J. Agric. Food Chem.* **2016,** 64, 371–380.
13. Wang, X.; Wu, P.; Hou, X.; Lv, Y. An ascorbic acid sensor based on protein-modified Au nanoclusters. *Analyst* **2013,** 138, 229-233.